Available online at www.sciencedirect.com

ScienceDirect

Scripta Materialia 60 (2009) 112–115

Scripta MATERIALIA

www.elsevier.com/locate/scriptamat

Friction stir welding of $Zr_{55}Cu_{30}Al_{10}Ni_5$ bulk metallic glass to Al–Zn–Mg–Cu alloy

D. Wang, B.L. Xiao, Z.Y. Ma* and H.F. Zhang

Shenyang National Laboratory for Materials Science, Institute of Metal Research, Chinese Academy of Sciences, 72 Wenhua Road, Shenyang 110016, China

Received 14 August 2008; revised 15 September 2008; accepted 16 September 2008
Available online 27 September 2008

$Zr_{55}Cu_{30}Al_{10}Ni_5$ bulk metallic glass (BMG) 1.7 mm thick and Al–Zn–Mg–Cu alloy plates were successfully joined by friction stir welding (FSW), producing defect-free BMG–Al joints. Some BMG particles were stirred into the aluminum side of the nugget zone; however, crystallization did not occur during FSW. No reaction layer was detected around the BMG particles and at the interface of two materials. The ultimate tensile strength (432 MPa) of the BMG–Al joint reached up to 74% of the base aluminum alloy.

Keywords: Friction stir welding; Metallic glasses; Aluminum; Fracture

Bulk metallic glasses (BMGs) exhibit high specific strength, hardness and superior corrosion resistance [1–3]. Although some BMGs can be fabricated directly from the melt due to high glass-forming capability, limitation on the size of the BMGs is a key issue for industrial applications [4,5]. Successful joining of BMGs has contributed to advancing the practical applications of the BMGs. In 2001, Kawamura et al. [6] succeeded in joining $Pd_{40}Ni_{40}P_{20}$ BMG by friction welding. Later, other welding methods, such as the electron beam welding, pulse-current or spark welding, and laser welding, were also successfully used to join BMGs [7–9]. However, it was reported that most welded amorphous alloys were embrittled by heat, leading to structural relaxation, phase separation and crystallization [8]. Therefore, for welding of BMGs, the heat input must be reduced to the minimum. Furthermore, the cooling must be also controlled within a critical cooling rate.

Joining BMGs to crystalline metallic materials is an important method for broadening the applications of the BMGs. Kawamura [10] and Kim et al. [11] investigated the electron beam welding of Zr and Ti to Zr-based BMGs, and defect-free joints were achieved with bending strengths higher than that of the crystalline metal. Kawamura [10] successfully welded commercial 5083 and 2017 aluminum alloys to $Zr_{41}Ti_{14}Cu_{12}Ni_{10}Be_{23}$ BMG by friction welding; however, he failed to weld 7075 aluminum alloy to the BMG due to the differing deformabilities of the 7075 alloy and the BMG in the friction welding process. Few studies on the welding of BMGs to commercial alloys have been reported to date. Therefore, it is worthwhile to investigate welding between BMGs and commercial light alloys by means of other welding techniques.

Friction stir welding (FSW) is a novel solid-state welding method, which has found particular applications in the aerospace and automotive industries. In FSW, localized heating due to friction between the tool and workpieces, and plastic deformation of material, softens the material around the pin, and the combination of tool rotation and translation results in movement of material from the front to the back of the pin, thereby producing a welded joint in the solid state [12]. Therefore, FSW is an ideal welding technique for joining BMGs together and for joining BMGs to crystalline metallic materials, with few limitations on the cooling rate in the welding process.

Aluminum alloys are widely used in the aerospace, automotive and marine industries. 7075 aluminum alloy, a commercial high-strength aluminum alloy, is widely used in structural applications [13]. In this paper, a bulk amorphous $Zr_{55}Cu_{30}Al_{10}Ni_5$ alloy and 7075 aluminum alloy were subjected to FSW to investigate possibility of joining the BMG to commercial high-strength aluminum alloys.

* Corresponding author. Tel.:/fax: +86-24-83978908; e-mail: zyma@imr.ac.cn

1359-6462/$ - see front matter © 2008 Acta Materialia Inc. Published by Elsevier Ltd. All rights reserved.
doi:10.1016/j.scriptamat.2008.09.014

Plates of $Zr_{55}Cu_{30}Al_{10}Ni_5$ BMG 1.7 mm thick and 7075-T651 aluminum alloy with a composition of Al–5.6Zn–2.5Mg–1.6Cu–0.23Cr (wt.%) were friction stir butt welded at a welding speed of 200 mm min^{-1} and a tool rotation rate of 600 rpm. The tool used had a shoulder 12 mm in diameter and a cylindrical pin 4 mm in diameter and 1.5 mm in length. The BMG was put on the advance side and the 7075 alloy on the retreating side. The tool pin was offset into the aluminum side with only 12.5% width of the pin in the BMG side during welding.

The joint was cross-sectioned perpendicular to the welding direction for optical microscopic (OM) examination and hardness measurement. The OM specimen was mechanically polished and etched by a solution of HF 0.5 ml, HNO_3 15.5 ml, H_2O 84 ml, CrO_3 3 g. The Vickers hardness profile of the weld was measured on the cross-section along the center line of the welded plate. Tensile specimens with a gauge length of 15 mm and width of 3 mm were machined perpendicular to the welding direction with the nugget zone (NZ) being in the center of the gauge. Thin foils for transmission electron microscopy (TEM) were cut from the NZ and thinned by ion milling. The foils were examined in a Phillip TECNAI G2 20 microscope.

Figure 1a shows a typical cross-sectional macrograph of the FSW BMG–7075 alloy joint. No defects were detected in the joint, indicating that the sound joining was achieved between the BMG and 7075 alloy by FSW. There was a clear interface between the BMG (the white zone on the advancing side) and the 7075 alloy (the gray zone on the retreating side). However, some particles of the BMG were detected in the 7075 alloy side near the interface, indicating that part of the BMG was broken into the particles and stirred into the aluminum matrix in the NZ during FSW.

Figure 2 illustrates the X-ray diffraction patterns of the BMG, the 7075 alloy and the joint. The as-received BMG is an amorphous alloy, as shown by curve a. By comparison, the 7075 alloy is characterized by the diffraction peaks of the aluminum and the metastable phase of η′ ($MgZn_2$) (marked by the solid circle in curve c), the main strengthening precipitate in 7075-T651 aluminum alloy [13]. For the FSW BMG–7075 alloy joint, as shown by curve b, in addition to the peaks of both the BMG and the 7075 alloy, no other peaks were detected, indicating that no crystallization of the BMG or reaction between the 7075 alloy and the BMG happened during FSW.

Figure 1b shows the TEM image of the NZ in the aluminum side near the interface. The grains in the NZ were equiaxial with a size of about 1–2 μm, which is much smaller than that (about 100 μm) of the base material. Intense deformation during FSW resulted in the recrystallization in the NZ, thereby refining the grains. This is similar to the previous reports [14].

Some small particles were detected in the NZ (marked as A in Figure 1b). Energy diffraction spectrum (EDS) analyses showed that this particle was a Zr-rich phase containing 38% Zr, 23% Cu, 4% Ni, 28% Al and 7% Zn (wt.%). The insert in Figure 1b is a diffraction pattern of particle A, which is a typical amorphous diffraction pattern. This indicated that particle A was scraped from the BMG and stirred into the NZ in the welding process and still maintained the amorphous structure. Furthermore, no reaction product was detected on the interface between particle A and the 7075 alloy. This indicated that no obvious reaction occurred between the BMG and 7075 alloy during FSW. Previously, Ohkubo et al. reported that there was a 30 nm thick reaction layer in the interface of the friction-welded $Pd_{40}Ni_{40}P_{20}$ and $Pd_{40}Cu_{30}Ni_{10}P_{20}$ BMG [15]. However, a 20 μm thick reaction layer was observed in the interface between Ti and a Zr-based BMG in an electron beam welded Ti–BMG joint [11]. These results indicate that the interfacial reaction during the welding depends on both the materials and the process.

Numerous fine particles with a size of about 100 nm were observed within the grains (Fig. 1b). For the 7075 alloy, the η phase partially remained in the NZ after FSW. Furthermore, a few Al_3Cr dispersoids existed in the 7075 alloy that did not dissolve during FSW [16]. On the other hand, the break-up of the BMG by the threaded pin might lead to the dissolution of some elements of the BMG into the 7075 alloy, thereby forming some different particles after FSW. Therefore, the fine particles within the NZ were very complex and more detailed microstructural investigation is needed.

Figure 3 illustrates the hardness profile of the joint on the 7075 alloy side. The zero point denotes the interface of the two materials and the distance from the zero indicates the interval from the tested point to the interface. The hardness profile for this FSW BMG–7075 alloy joint is quite similar to that for the FSW 7075-T651 joint [17]. The hardness of the FSW BMG–7075 alloy joint was lower than that of the 7075-T651 base alloy (∼180 Hv). For 7000 series alloys, the high strength of the alloys is due to the strengthening precipitates in the matrix [14,16]. When the alloys are welded by FSW, the precipitates in both the NZ and HAZ will coarsen and/or dissolve, resulting in reduced hardness. However, the significant grain refinement by recrystallization tends to increase the hardness of the NZ. In this case, the HAZ has the lowest hardness and most of FSW 7000 alloy joints failed in the HAZ during the transverse tensile test.

The ultimate tensile strength of the joint is 423 MPa and reaches up to 74% of the 7075-T651 alloy. The joint efficiency is close to that (75%) for the FSW 7075-T651 joint [17]. The joint failed in the NZ on the aluminum side, ∼1.6 mm from the BMG–7075 alloy interface (not shown). This indicates that the bonding strength of the interface between the BMG and 7075 alloy was excellent. However, unlike the FSW 7075-T651 alloy joint, the FSW BMG–7075 alloy joint in this study did not fail in the HAZ, i.e. the lowest hardness regions, as shown in Figure 3. This implies that the NZ on the aluminum side was weaker than the HAZ for this FSW BMG–7075 alloy joint during the tensile test.

SEM micrographs of the tensile fracture surface of the joint are shown in Figure 4. In the macrograph, some huge particles were observed on the fracture surface, as shown by points A and B in Figure 4a. EDS analyses indicated that point B contained 57% Zr, 15% Cu, 3%

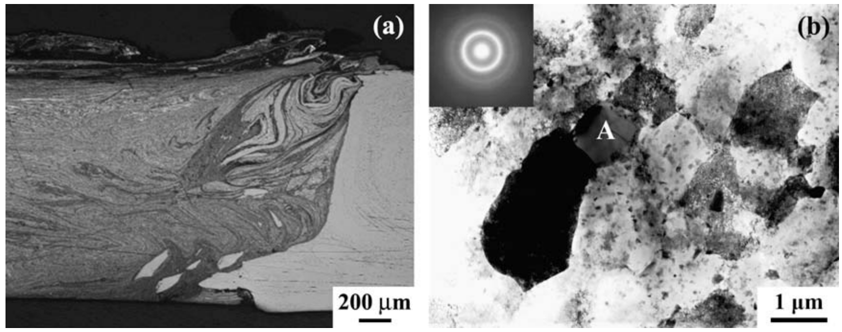

Figure 1. (a) Optical micrographs showing the cross-section across the interface of FSW BMG and 7075 alloy, and (b) a TEM image showing fine grains and BMG particles in the 7075 side near the BMG–alloy interface (inserted micrograph shows diffraction pattern of zone A).

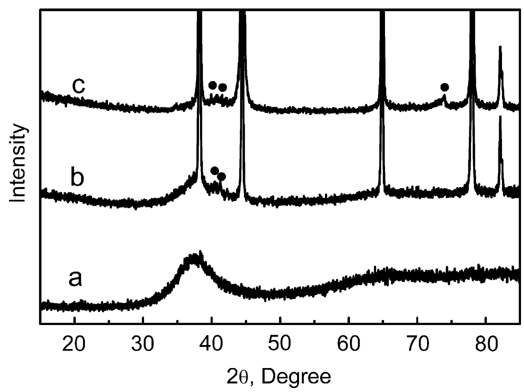

Figure 2. X-ray diffraction pattern of (a) BMG, (b) cross-section of joint, (c) 7075 alloy.

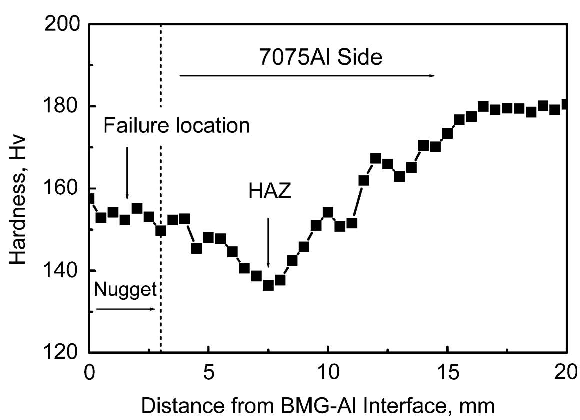

Figure 3. Hardness profiles of FSW BMG–7075 alloy joint in the 7075 side.

Ni, 24% Al and 1%Mg (wt.%). Similarly, other particles on the fracture surface were also determined to be Zr-rich particles. A magnified view of region B marked in Figure 4a is shown in Figure 4b, and for the purpose of comparison, the same region on the other side of the failed tensile specimen is shown in Figure 4c. From Figure 4b and c it is clear that the BMG particles in the NZ, which were stirred to the aluminum matrix during FSW, were fractured in the tensile process. The other regions of the fracture surface were characterized by large dimples and tearing ridges which were similar to the fracture surfaces observed in the FSW 7075 alloy joint [16,17]. During the tensile test, the large hard and brittle BMG particles in the NZ induced nonuniform deformation of 7075 alloy, and these large particles were firstly fractured at relatively low stress due to the load transfer from the matrix. In this case, the tensile properties of the joint were somewhat deteriorated. Therefore, although the softest region in the FSW BMG–7075 alloy joint was the HAZ, the sample fractured in the NZ.

Mahoney et al. [16] measured the peak temperature distribution during FSW of 7075-T651 alloy. They found that the temperatures adjacent to the NZ were 420–470 °C. According to the previous reports, the glass transition temperature (T_g) of $Zr_{55}Cu_{30}Al_{10}Ni_5$ is about 410 °C and the crystallization temperature (T_c) is about 494 °C [3]. Furthermore, no crystallization of the BMG was detected in the NZ, as shown in Figure 2. Therefore, the temperature of the NZ during FSW should be lower than the T_c and higher than the T_g. Furthermore, some researchers reported that BMGs displayed Newtonian viscosity, usually described by the Vogel–Fulcher–Tammann formula in the supercooled liquid region [18]. Although the effective viscosity decreased smoothly with increasing temperature, the T_c of the BMGs was almost unaffected by the extrusion process. On the other hand, Kobata et al. [19] reported the friction stir processing of $Zr_{55}Cu_{30}Al_{10}Ni_5$ BMG, which was a process similar to FSW of a single plate. Some nanoscale structure bands, but no crystallization, were found in the NZ, indicating that the serious deformation in the NZ did not lead to the crystallization of the BMG. Therefore, it can be concluded that in the FSW process, both BMG and 7075 alloy were heated above the T_g temperature of the BMG; however, the heat input generated by the friction and serious deformation were not enough to crystallize the BMG. The wonderful fluidity of the BMG in the supercooled liquid region was beneficial to the mixing of the BMG with the 7075 alloy and finally the welding beam was formed without defect and crystallization.

In summary, the following conclusions are reached:

(1) A defect-free FSW $Zr_{55}Cu_{30}Al_{10}Ni_5$ BMG and 7075-T651 alloy joint was successfully achieved by offsetting the pin to the aluminum side.
(2) The NZ consisted of fine recrystallized aluminum grains with some BMG particles being stirred into the aluminum matrix. No crystallization of the

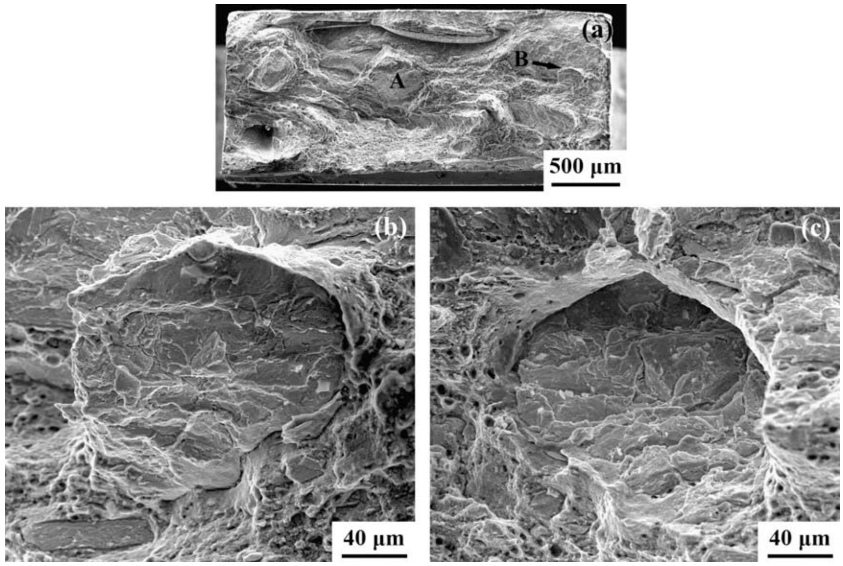

Figure 4. SEM image showing tensile fracture surfaces of FSW joint: (a) macrograph of fracture surface, (b) magnified view of zone B in (a), and (c) the same region as in (b) from other side of a failed specimen.

BMG and reaction layer around the BMG particles and between BMG/aluminum interfaces were detected.

(3) The strength of the FSW BMG–7075 alloy joint reached up to 74% of the 7075-T651 alloy with the joint failing in the NZ on the aluminum side, indicating that while the interface between BMG and 7075 alloy had an excellent bonding, the large BMG particles in the NZ reduced the strength of the joint somewhat.

This work was supported by the National Outstanding Young Scientist Foundation for Z.Y.M. under Grant No. 50525103, the National Basic Research Program of China under Grant Nos. 2006CB605205 and 2006CB605201, and the Hundred Talents Program of the Chinese Academy of Sciences.

[1] A. Inoue, Acta Mater. 48 (2000) 279.
[2] A. Peker, W.L. Johnson, Appl. Phys. Lett. 63 (1993) 2342.
[3] A. Inoue, T. Zhang, Mater. Trans. 37 (1996) 185.
[4] Y. Kawamura, T. Shoji, Y. Ohno, J. Non-Cryst. Solids 317 (2003) 152.
[5] T. Shoji, Y. Kawamura, Y. Ohno, Mater. Sci. Eng. 375–377 A (2004) 394.
[6] Y. Kawamura, Y. Ohno, Scripta Mater. 45 (2001) 279.
[7] Y. Yokoyama, N. Abe, K. Fukaura, T. Shinohara, A. Inoue, Mater. Sci. Eng. 375–377 A (2004) 422.
[8] A.J. Swiston, E. Besnoin, A. Duckham, O.M. Knio, T.P. Weihs, T.C. Hufnagel, Acta Mater. 53 (2005) 3713.
[9] B. Li, Z.Y. Li, J.G. Xiong, L. Xing, D. Wang, Y. Li, J. Alloy Compd. 413 (2006) 118.
[10] Y. Kawamura, Mater. Sci. Eng. 375–377 A (2004) 112.
[11] J. Kim, Y. Kawamura, Scripta Mater. 56 (2007) 709.
[12] R.S. Mishra, Z.Y. Ma, Mater. Sci. Eng. R 50 (2005) 1.
[13] J.E. Hatch (Ed.), Aluminum Properties and Physical Metallurgy, American Society for Metals, Materials Park, OH, 1984.
[14] J.Q. Su, T.W. Nelson, R. Mishra, M. Mahoney, Acta Mater. 51 (2003) 713.
[15] T. Ohkubo, S. Shoji, Y. Kawamura, K. Hono, Scripta Mater. 53 (2005) 493.
[16] M.W. Mahoney, C.G. Rhodes, J.G. Flintoff, R.A. Spurling, W.H. Bingel, Metall. Mater. Trans. 29A (1998) 1955.
[17] S.R. Ren, Z.Y. Ma, L.Q. Chen, Mater. Sci. Eng. 479A (2008) 293.
[18] A. Inoue, Y. Kawamura, T. Shibata, K. Sasamori, Mater. Trans. 37 (1996) 1337.
[19] J. Kobata, Y. Takigawa, S.W. Chung, H. Tsuda, H. Kimura, K. Higashi, Mater. Lett. 61 (2003) 3771.